Australian Government
Department of Defence
Defence Science and
Technology Organisation

Thermodynamically Consistent Decoupled Strength Model for Two-Phase Materials with Phase Transitions

A.D. Resnyansky

Weapons Systems Division
Defence Science and Technology Organisation

DSTO-TR-2367

ABSTRACT

A constitutive two-phase material model is formulated, which satisfies the decoupling of deviatoric stress and pressure response required by many hydrocodes. Two-phase materials are assumed to be non-dispersive. Basis of the present model is a decoupled model based on a general Maxwell-type viscoelastic model. The proposed formulation provides thermodynamic consistency for the case of small elastic shear strains and unrestricted volumetric response. The model is verified against experimental data on the shock wave propagation in iron resulting in alpha-epsilon phase transition, while the strength effects being observed at the same time.

Published by

Weapons Systems Division
DSTO Defence Science and Technology Organisation
PO Box 1500
Edinburgh South Australia 5111 Australia

Telephone: (08) 8259 5555
Fax: (08) 8259 6567

AR-014-677
December 2009

APPROVED FOR PUBLIC RELEASE

Thermodynamically Consistent Decoupled Strength Model for Two-Phase Materials with Phase Transitions

Executive Summary

In order to increase the efficiency of modern weapons and protection systems, novel technology developments deal with advanced multi-phase and multi-component materials. Among them are filled energetic materials, porous and multi-phase mitigants, composite materials, including nano-ceramics, etc. Behaviour and response of a variety of multi-phase non-dispersive materials, including porous and condensed phase-transforming multi-phase materials, has to be described in order to enhance the technology. This poses new challenges in the area of constitutive multi-phase modelling of the material response at extreme conditions. Advanced numerical codes are employed, amongst which hydrocodes are particularly suitable because they may model the material behaviour in a wide range of conditions from moderate impact and blast loads resulting in the strength-sensitive response till extreme explosion and hypervelocity impact loads resulting in the strength negligible response. From the physical mechanism of deformation viewpoint, the moderate loads are associated with the elasto-plastic deformation / transition and the extreme loads are associated with the hydrodynamic material flows at extreme pressures and temperatures. The elasto-plastic response in the defence applications is needed to be constitutive (i.e., it should take into account the rate sensitivity of the yield stress) and requires advanced models. At present, the multi-phase material models, which describe both the strength effects and the extreme hydrodynamic behaviour, are rare. Therefore, development and implementation of advanced models in commercially available hydrocodes is a great challenge. The modelling capability in DSTO is supported by two major hydrocodes, LS-DYNA3D and CTH. Hydrocode LS-DYNA3D proved its efficiency for the material response to moderate deformations when a good resolution of contact interfaces is required. However, for the problems such as counter-IED (Improvised Explosive Devices) designs, where intensive flows, large deformations, and multi-phase mix-up are common, a Eulerian code such as CTH is better suited for this model. Both codes require material models decoupling the volumetric and shear response, which are not common for the majority of thermodynamically consistent models dealing with the wide range of loads.

Recently, a decoupled model that describes both the strength effects and hydrodynamic behaviour of condensed materials has been developed in DSTO [1]. However, the model [1] is dealing only with single phase materials. The present work extends the model to the case of two-phase materials. The model is verified against experimental data on the shock response of iron resulting in the alpha-epsilon phase transition. At the same time, the strength-level response is observed as a multi-step shock wave structure with the steps corresponding to both the alpha-epsilon transition

and the elasto-plastic transition (elastic precursor). The modelling results correlate well with the experimental results available in literature.

Reference

[1] Resnyansky A.D., Thermodynamically Consistent Decoupled Shear-Volumetric Strain Model and CTH Implementation, DSTO Report DSTO-TR-2299, Edinburgh, SA, Australia, 2009.

Authors

A.D. Resnyansky
Weapons Systems Division

Anatoly Resnyansky obtained an MSc in Applied Mathematics and Mechanics from Novosibirsk State University (Russia) in 1979. In 1979-1995 he worked in the Lavrentyev Institute of Hydrodynamics (Russian Academy of Science) in the area of constitutive modelling for problems of high-velocity impact. Anatoly obtained a PhD in Physics and Mathematics from the Institute of Hydrodynamics in 1985. In 1996-1998 he worked in private industry in Australia. He joined the Weapons Effects Group of the Weapons Systems Division (DSTO) in 1998. His current research interests include constitutive modelling and material characterisation at high strain rates, ballistic testing and simulation, and theoretical and experimental analysis of multi-phase flows. He has more than eighty papers published internationally in this area.

Contents

1. Introduction

A large number of advanced multi-phase and strength material models have been developed in the last decades. Many of the models have been implemented in commercial hydrocodes such as LS-DYNA [1] and CTH [2]. Many of the strength models have a decoupled representation separating the volumetric (bulk) response managed by hydrostatic pressure from the deviatoric response managed by the shear stresses. A number of advanced strength models that are attractive from their thermodynamic consistency, however, are not decoupled and cannot be directly used for the hydrocode implementation. In order to keep the thermodynamic correctness, a revision of one of the models [3] has recently been conducted and a decoupled strength model has been developed [4] and implemented in the CTH hydrocode.

The present work generalises the model [4] to the case of two-phase non-dispersive materials. Such materials have components/phases with the particle velocities equilibrated over the multi-phase mixture. Examples of these materials are numerous and include porous materials, liquids with bubbles, reaction products of energetic materials with particles small enough to achieve almost instantaneous equilibrium by velocity, phase-transforming two-phase condensed materials, etc. The present extensions of the model [4] for the case of small elastic shear deformations and unrestricted bulk response focuses on 1) formulation of the model into the form that is in agreement with the hydrocode implementation decoupling convention; and 2) checking out the thermodynamic correctness of the model.

Formulation of the model is based on two major points: i) a choice of thermodynamic variables and ii) derivation of constitutive equations and conservation laws. The closing relations, including the equation of state (EOS), are obtained naturally from the corresponding relations for individual phases. While implementing the model, a one-dimensional in-house wave propagation code has been developed employing the Godunov method [5] on the basis of the Riemann problem procedure [6] for the bulk response and a linearised method similar to the method of characteristics for the shear response.

The model is verified against data available in literature on the velocity of the free surface of iron target in the plate impact experiments at using the shock propagation basic set-up for shock compression of pure iron. The calculations demonstrate both alpha-epsilon (bcc-to-hcp) phase transition and elastic precursor development (the elasto-plastic transition), which agrees well with the experiments.

2. Background Constitutive Model

The Maxwell-type viscoelastic model [3] reduced to the case of small shear elastic deformations is used in the following form [4]:

$$\frac{\partial \rho e_{ij}}{\partial t}+\frac{\partial \rho u_k e_{ij}}{\partial x_k}-\frac{\partial u_i/2}{\partial x_j}-\frac{\partial u_j/2}{\partial x_i}+\frac{\partial u_k/3}{\partial x_k}\cdot\delta_{ij}=-\frac{\rho e_{ij}}{\tau}\,.$$

$$\frac{\partial \rho}{\partial t}+\frac{\partial \rho u_k}{\partial x_k}=m_0\,,\quad \frac{\partial \rho u_i}{\partial t}+\frac{\partial\left(\rho u_i u_j-s_{ij}\right)}{\partial x_j}+\frac{\partial p}{\partial x_i}=n_0^i\,, \tag{1}$$

$$\frac{\partial \rho\left(e+u^2/2\right)}{\partial t}+\frac{\partial\left[\rho u_j\left(e+u^2/2\right)-s_{ij}u_i+pu_j\right]}{\partial x_j}=l_0\,.$$

The equations are written down in the Eulerian coordinate system in the form of the balance laws with external exchange terms. The source terms of the external flows m_0, n^i_0, and l_0 are zero (turning the balance laws to the conservation laws) for the original single phase model [4] describing a closed material system. We will denote the substantial derivative $d/dt = \partial/\partial t + u_k \cdot \partial/\partial x_k$. The prime sign will refer a tensor to its deviatoric part, so $\varepsilon'_{ij} = \varepsilon_{ij} - \varepsilon_{kk}\cdot\delta_{ij}/3$, where δ_{ij} are components of the unit tensor. Here $e_{ij} = \varepsilon'_{ij}/\rho$ where ε_{ij} and s_{ij} are components of the tensor of small elastic deformations and deviatoric stress tensor, u_i are velocity components, and ρ and e are density and specific internal energy. The velocity module u is determined as $u^2 = u_i \cdot u_i$. The deviatoric part s_{ij} of the stress tensor σ_{ij} and the spherical (negative) part p of the stress tensor (pressure) are linked as follows

$$s_{ij} = \sigma_{ij} + p\cdot\delta_{ij}\quad,\quad p = -\sigma_{kk}/3\ . \tag{2}$$

Pre-given functions $\tau(\varepsilon_{ij}, T)$ and $e(\rho, e_{ij}, s)$, where T and s are temperature and specific entropy, close the system of equations of the model. The function $\tau(\varepsilon_{ij}, T)$ is obtained from the data on yield limit versus strain rate (e.g., see [7] on how this can be done) and the internal energy $e(\rho, e_{ij}, s)$ is obtained from high-pressure material response data such as Hugoniots or static compression data.

The thermodynamic identity (3) for the present model (see [4]) is:

$$T\,ds = de - s_{ij}\,de_{ji} + p\,dV, \tag{3}$$

where $V = 1/\rho$ is the specific volume. Thus, we have 11 independent thermodynamic variables, namely, e_{ij}, ρ, and s and 11 dependent variables: s_{ij}, p, and T. The dependent variables are calculated from the identity (3) as follows:

$$T = \partial e/\partial s\ ,\quad p = \rho^2\partial e/\partial\rho\ ,\quad s_{ij} = \partial e/\partial e_{ji}\ . \tag{4}$$

From the symmetry conditions for the strain and stress tensors and from the following deviatoric conditions for tensor deviators: $e_{11} + e_{22} + e_{33} = 0$ and $s_{11} + s_{22} + s_{33} = 0$, the number of variables to be calculated is reduced to 10; this set includes the thermodynamic variables and velocity components.

3. Thermodynamic Variables

For a two-phase material the phases are characterised by density ρ, small elastic deviatoric deformations e_{ij}, specific entropy s, plus pressure p, deviatoric stresses s_{ij}, and temperature T; the second half of the variables are dependent thermodynamic variables. Velocity u is the same for both phases in the non-dispersive materials. Variables for the corresponding phases 1 or 2 are referred by superscripts in parentheses. Both phases are assumed to be compressible and to have individual strength and other material properties. The volume and mass concentrations of the first phase are θ and c; they are defined identically to the definitions from [6, 8-10] with similar relations for averaged density ρ, entropy s, pressure p, and internal energy e :

$$\rho = \theta\,\rho^{(1)} + (1-\theta)\,\rho^{(2)}\,, \quad p = \rho^2 e_\rho = \theta\,p^{(1)} + (1-\theta)\,p^{(2)}\,,$$
$$e = c\,e^{(1)} + (1-c)\,e^{(2)}\,, \quad s = c\,s^{(1)} + (1-c)\,s^{(2)}\,. \tag{5}$$

For deformations we assume that the deformations for mixture should be volume averaged similarly to [11-13]:

$$\varepsilon'_{ij} = \theta\,\varepsilon'^{(1)}_{ij} + (1-\theta)\,\varepsilon'^{(2)}_{ij}\,.$$

Then, using the relation [4] $\varepsilon'_{ij} = \rho e_{ij}$ and the definitions [6, 8-10]

$$\rho^{(1)} = \rho\,c/\theta\,, \quad \rho^{(2)} = \rho(1-c)/(1-\theta)\,, \tag{6}$$

we have

$$e_{ij} = c\,e^{(1)}_{ij} + (1-c)\,e^{(2)}_{ij}\,. \tag{7}$$

Inter-phase deformation imbalance λ_{ij} is introduced as follows: $\rho\lambda_{ij} = \varepsilon'^{(1)}_{ij} - \varepsilon'^{(2)}_{ij}$, which results in

$$\lambda_{ij} = c\,e^{(1)}_{ij}/\theta - (1-c)\,e^{(2)}_{ij}/(1-\theta)\,. \tag{8}$$

The entropy disequilibrium is introduced in the way used in [6, 9]:

$$\chi = c\,s^{(1)} - (1-c)\,s^{(2)}\,. \tag{9}$$

The definitions (6) and (9) enable us to link phase entropies and densities with corresponding averaged variables. Following these definitions, we can express the independent phase state variables via the averaged ones as follows:

$$\rho^{(1)} = \rho\,c/\theta\,,\ \rho^{(2)} = \rho(1-c)/(1-\theta)\,,\ s^{(1)} = \tfrac{1}{2}(s+\chi)/c\,,\ s^{(2)} = \tfrac{1}{2}(s-\chi)/(1-c)\,. \tag{10}$$

Similarly, the link between $e^{(1)}_{ij}$, $e^{(2)}_{ij}$, and e_{ij} is

$$e_{ij}^{(1)} = \theta\,(e_{ij} + \lambda_{ij}\,(1 - \theta\,))\,/\,c\,,\;\; e_{ij}^{(2)} = (1 - \theta\,)\,(e_{ij} - \lambda_{ij}\,\theta)\,/\,(1 - c)\,. \tag{11}$$

We assume that the internal energy dependencies, EOSs, for each phase are given in the form

$$e^{(1)} = e^{(1)}\big(\rho^{(1)},\, e_{ij}^{(1)},\, s^{(1)}\big)\quad,\quad e^{(2)} = e^{(2)}\big(\rho^{(2)},\, e_{ij}^{(2)},\, s^{(2)}\big)\;. \tag{12}$$

Thus, the averaged internal energy from (5) and (12) is a function of the following parameters:

$$\begin{aligned} e(\rho,\, c,\, \theta,\, e_{ij},\, \lambda_{ij},\, s,\, \chi) &= c\; e^{(1)}\,\big(\,\rho c/\theta,\, \theta(e_{ij} + \lambda_{ij}(1-\theta\,))/c,\, \tfrac{1}{2}(s + \chi)/c\big) + \\ &+ (1 - c)\; e^{(2)}\,\big(\,\rho(1-c)/(1-\theta\,),\, (1 - \theta)(e_{ij} - \lambda_{ij}\theta)/(1 - c),\, \tfrac{1}{2}(s - \chi)/(1 - c)\big)\quad, \end{aligned} \tag{13}$$

here the relations (10) and (11) have been used. Summarising, the independent variables that fully describe the strength bearing two-phase material are ρ, s, u, c, θ, e_{ij}, λ_{ij}, and χ. For this set of independent variables the thermodynamic identity takes the following form:

$$T\,ds = \;de + p\,dV - s_{ij}\,de_{ji} - Q_{ij}\,d\lambda_{ji} - \Lambda\,dc - \Pi\,d\theta - \Psi\,d\chi\;. \tag{14}$$

Thermodynamic identities for the phases can be used for calculation of averaged dependent variables from (14) as follows:

$$\begin{aligned} &p = \rho^2 e_\rho = \rho^2\Big(ce^{(1)} + (1-c)e^{(2)}\Big)_\rho = \theta\, p^{(1)} + (1-\theta)p^{(2)},\\ &s_{ij} = e_{e_{ji}} = \Big(ce^{(1)} + (1-c)e^{(2)}\Big)_{e_{ji}} = \theta\, s_{ij}^{(1)} + (1-\theta)s_{ij}^{(2)},\\ &T = e_s = \Big(ce^{(1)} + (1-c)e^{(2)}\Big)_s = cT^{(1)}\Big(s^{(1)}\Big)_s + (1-c)T^{(2)}\Big(s^{(2)}\Big)_s = \Big(T^{(1)} + T^{(2)}\Big)/2\,. \end{aligned} \tag{15}$$

Here, the chain rule and definition (13) have been employed when differentiating over averaged independent variables. The dependent thermodynamic variable Λ in (14) that is responsible for the change of phase mass is traditionally related to a chemical potential. Similarly to (15), when applying derivatives over c, λ_{ji}, θ, and χ to the internal energy e in (13), we have

$$\begin{aligned} &\Lambda = e_c = e^{(1)} + \frac{p^{(1)}}{\rho^{(1)}} - T^{(1)}s^{(1)} - e_{ij}^{(1)}s_{ij}^{(1)} - e^{(2)} - \frac{p^{(2)}}{\rho^{(2)}} + T^{(2)}s^{(2)} + e_{ij}^{(2)}s_{ij}^{(2)} = \mu_1 - \mu_2,\\ &Q_{ij} = e_{\lambda_{ji}} = \theta\,(1-\theta)\Big(s_{ij}^{(1)} - s_{ij}^{(2)}\Big),\\ &\Pi = e_\theta = -\frac{p^{(1)} - p^{(2)}}{\rho} + \Big[e_{ij} + (1-2\theta)\lambda_{ij}\Big]\Big(s_{ij}^{(1)} - s_{ij}^{(2)}\Big)\\ &\Psi = e_\chi = \Big(T^{(1)} - T^{(2)}\Big)/2\,. \end{aligned} \tag{16}$$

Here $\mu_k = e^{(k)} + p^{(k)}/\rho^{(k)} - T^{(k)}s^{(k)} - e_{ij}^{(k)}s_{ij}^{(k)}$ is the Gibbs energy for k-th phase and, thus, the chemical potential Λ associated with the mass concentration change is proportional to the affinity of the Gibbs energy. The potentials Q_{ij} and Ψ associated with the variations of the

strain imbalance λ_{ij} and the entropy disequilibrium χ are proportional to the affinities of the deviatoric stresses s_{ij} and temperature T. From (16), the potential Π associated with the variation of the volume concentration can be rewritten as follows

$$\Pi = e_\theta = -\frac{p^{(1)} - p^{(2)}}{\rho} + \left[e_{ij} + (1-2\theta)\lambda_{ij} \right]\left(s_{ij}^{(1)} - s_{ij}^{(2)} \right) =$$

$$= -\frac{p^{(1)} - p^{(2)}}{\rho} + \frac{s_{ij}^{(1)}\left(\rho^{(1)} e_{ij}^{(1)} \right) - s_{ij}^{(2)}\left(\rho^{(2)} e_{ij}^{(2)} \right)}{\rho} - \lambda_{ij} s_{ij} = \Pi_0 - \lambda_{ij} s_{ij} \, .$$

This means that the corresponding affinity is linked with the pressure affinity and with the affinities for the work of elastic shear strains and that for the strain (the last affinity is simply the strain imbalance). Using the definition of the strain imbalance, the last expression can be rewritten as follows

$$\Pi = e_\theta = -\frac{p^{(1)} - \left(\rho^{(1)} e_{ij}^{(1)} \right)\left(s_{ij}^{(1)} - s_{ij} \right) - p^{(2)} + \left(\rho^{(2)} e_{ij}^{(2)} \right)\left(s_{ij}^{(2)} - s_{ij} \right)}{\rho}.$$

Thus, the volume change associated potential Π is proportional to the pressure affinity and the affinity of $(\rho^{(k)} e_{ij}^{(k)})\cdot(s_{ij}^{(k)} - s_{ij})$ that is the shear strain work of the fluctuations of the deviatoric stresses over the averaged stresses.

4. Two-Phase Constitutive Model

In order to derive differential equations of the model, we will employ the equations (1) of the background model to the individual phases. In doing so, the source (exchange) terms that are denoted for the first phase by m_0, n^i_0, and l_0 will be replaced by $-m_0$, $-n^i_0$, and $-l_0$ for the second phase. This provides the balance of mass, momentum, and energy in the closed two-phase material system. For a representative volume containing several phases, the density and pressure are characterised by partial densities $\rho^{(1)\mathrm{P}} = \rho\cdot c = \theta\cdot\rho^{(1)}$ and $\rho^{(2)\mathrm{P}} = \rho\cdot(1-c) = (1-\theta)\cdot\rho^{(2)}$, and by partial pressures $p^{(1)\mathrm{P}} = \theta\cdot p^{(1)}$ and $p^{(1)\mathrm{P}} = (1-\theta)\cdot p^{(2)}$ (see [9]). The pressures are obtained from (4) for each phase, where partial densities are replacing the actual densities $\rho^{(1)}$ and $\rho^{(2)}$ in EOS. Similarly, partial characteristics for deformations and stresses can be introduced, resulting in $e_{ij}^{(1)\mathrm{P}} = e_{ij}^{(1)}/\theta$, $e_{ij}^{(2)\mathrm{P}} = e_{ij}^{(2)}/(1-\theta)$, and $s_{ij}^{(1)\mathrm{P}} = \theta\cdot s_{ij}^{(1)}$, $s_{ij}^{(2)\mathrm{P}} = (1-\theta)\cdot s_{ij}^{(2)}$.

Summing up the mass, momentum, and energy balance laws (1) for the first and second phase, we have

$$\frac{\partial \rho}{\partial t}+\frac{\partial \rho u_k}{\partial x_k}=0\,,\quad \frac{\partial \rho u_i}{\partial t}+\frac{\partial\left(\rho u_i u_j-s_{ij}\right)}{\partial x_j}+\frac{\partial p}{\partial x_i}=0\,,$$
$$\frac{\partial \rho\left(e+u^2/2\right)}{\partial t}+\frac{\partial\left[\rho u_j\left(e+u^2/2\right)-s_{ij}u_i+pu_j\right]}{\partial x_j}=0\,. \tag{17}$$

For the volume concentration θ the constitutive equation is taken in the following traditional form

$$\frac{\partial \rho\theta}{\partial t}+\frac{\partial \rho\theta u_j}{\partial x_j}=-\rho\psi\,. \tag{18}$$

Equation (18) can also be rewritten as $d\theta/dt = -\psi$ with the use of the mass conservation law from (17).

Using mass balance equation for the partial density $\rho^{(1)p} = \rho\cdot c$ of the first phase, we can associate the rate of change of the mass concentration parameter c with a rate function φ. Thus, the continuity equation for $\rho^{(1)p}$ gives:

$$\frac{\partial \rho c}{\partial t}+\frac{\partial \rho c u_j}{\partial x_j}=-\rho\varphi\,. \tag{19}$$

From the constitutive equation for c of (1), it is obvious that $m_0 = -\rho\varphi$. Using equations (19) and (18), we can derive auxiliary equations for $\rho^{(1)}$ and $\rho^{(2)}$:

$$\frac{\partial \rho^{(1)}}{\partial t}+\frac{\partial \rho^{(1)}u_j}{\partial x_j}=\frac{m_0+\rho^{(1)}\psi}{\theta}\,,\quad \frac{\partial \rho^{(2)}}{\partial t}+\frac{\partial \rho^{(2)}u_j}{\partial x_j}=-\frac{m_0+\rho^{(2)}\psi}{1-\theta}. \tag{20}$$

The equations (20) are needed for derivation of constitutive equations for strains and strain imbalances. In particular, the strain constitutive equations from (1) for the phases are

$$\frac{\partial \rho^{(1)p}e_{ij}^{(1)p}}{\partial t}+\frac{\partial \rho^{(1)p}u_k e_{ij}^{(1)p}}{\partial x_k}-\frac{\partial u_i/2}{\partial x_j}-\frac{\partial u_j/2}{\partial x_i}+\frac{\partial u_k/3}{\partial x_k}\cdot\delta_{ij}=-\frac{\rho^{(1)p}e_{ij}^{(1)p}}{\tau_1}\,,$$
$$\frac{\partial \rho^{(2)p}e_{ij}^{(2)p}}{\partial t}+\frac{\partial \rho^{(2)p}u_k e_{ij}^{(2)p}}{\partial x_k}-\frac{\partial u_i/2}{\partial x_j}-\frac{\partial u_j/2}{\partial x_i}+\frac{\partial u_k/3}{\partial x_k}\cdot\delta_{ij}=-\frac{\rho^{(2)p}e_{ij}^{(2)p}}{\tau_2}\,. \tag{21}$$

Keeping in mind that $\rho^{(1)p}e_{ij}^{(1)p} = \rho^{(1)}e_{ij}^{(1)}$ and $\rho^{(2)p}e_{ij}^{(2)p} = \rho^{(2)}e_{ij}^{(2)}$, and using (20), from (21) we have:

$$
\begin{aligned}
&e_{ij}^{(1)}\left(\frac{m_0+\rho^{(1)}\psi}{\theta}\right)+\rho^{(1)}\frac{de_{ij}^{(1)}}{dt}-\frac{\partial u_i/2}{\partial x_j}-\frac{\partial u_j/2}{\partial x_i}+\frac{\partial u_k/3}{\partial x_k}\cdot\delta_{ij}=-\frac{\rho^{(1)}e_{ij}^{(1)}}{\tau_1}=-\varphi_{ij}^{(1)}\ ,\\
&-e_{ij}^{(2)}\left(\frac{m_0+\rho^{(2)}\psi}{1-\theta}\right)+\rho^{(2)}\frac{de_{ij}^{(2)}}{dt}-\frac{\partial u_i/2}{\partial x_j}-\frac{\partial u_j/2}{\partial x_i}+\frac{\partial u_k/3}{\partial x_k}\cdot\delta_{ij}=-\frac{\rho^{(2)}e_{ij}^{(2)}}{\tau_2}=-\varphi_{ij}^{(2)}\ .
\end{aligned}
\tag{22}
$$

Now, we can reduce (22) if multiplying the equations from (22) by $\rho c/\rho^{(1)}$ and $\rho(1-c)/\rho^{(2)}$, respectively, and summing them up separately with equation (19) for c (with m_0 replacing the right hand side) multiplied by $e_{ij}^{(1)}$ and with a similar equation for $1-c$ multiplied by $e_{ij}^{(2)}$, respectively. Using (6), the resulting equations are

$$
\begin{aligned}
&\frac{\partial\rho ce_{ij}^{(1)}}{\partial t}+\frac{\partial\rho ce_{ij}^{(1)}u_k}{\partial x_k}-\theta\left(\frac{\partial u_i/2}{\partial x_j}-\frac{\partial u_j/2}{\partial x_i}+\frac{\partial u_k/3}{\partial x_k}\cdot\delta_{ij}\right)=-\frac{\rho ce_{ij}^{(1)}}{\tau_1}-\rho^{(1)}e_{ij}^{(1)}\psi\ ,\\
&\frac{\partial\rho(1-c)e_{ij}^{(2)}}{\partial t}+\frac{\partial\rho(1-c)e_{ij}^{(2)}u_k}{\partial x_k}-\\
&-(1-\theta)\left(\frac{\partial u_i/2}{\partial x_j}-\frac{\partial u_j/2}{\partial x_i}+\frac{\partial u_k/3}{\partial x_k}\cdot\delta_{ij}\right)=-\frac{\rho(1-c)e_{ij}^{(2)}}{\tau_2}+\rho^{(2)}e_{ij}^{(2)}\psi\ .
\end{aligned}
\tag{23}
$$

Summing up equations of (23) and using (7), we have a constitutive equation for e_{ij}:

$$
\frac{\partial\rho e_{ij}}{\partial t}+\frac{\partial\rho e_{ij}u_k}{\partial x_k}-\frac{\partial u_i/2}{\partial x_j}-\frac{\partial u_j/2}{\partial x_i}+\frac{\partial u_k/3}{\partial x_k}\cdot\delta_{ij}=-\left(\theta\varphi_{ij}^{(1)}+(1-\theta)\varphi_{ij}^{(2)}\right)-\rho\lambda_{ij}\psi\ ,
\tag{24}
$$

here the notations from (22): $\varphi_{ij}^{(1)}=\rho\,[e_{ij}+(1-\theta)\,\lambda_{ij}]/\tau_1$ and $\varphi_{ij}^{(2)}=\rho\,[e_{ij}-\theta\,\lambda_{ij}]/\tau_2$ are used. Direct subtraction of the second equation from the first one in (21) gives the following constitutive equation for the parameter λ_{ij} defined in (8)

$$
\frac{\partial\rho\lambda_{ij}}{\partial t}+\frac{\partial\rho\lambda_{ij}u_k}{\partial x_k}=-\left(\varphi_{ij}^{(1)}-\varphi_{ij}^{(2)}\right).
\tag{25}
$$

Derivation of a constitutive equation for χ is conducted similarly to [9]. Specifically, we use the energy equations for phases that take the following form after reductions with mass and momentum balance laws

$$\rho^{(1)p}\frac{\partial e^{(1)}}{\partial t}+p^{(1)p}\frac{\partial u_k}{\partial x_k}-s_{ij}^{(1)p}\frac{\partial u_j}{\partial x_i}=l_0-u_k n_0^k-m_0\left(e^{(1)}-u^2\Big/2\right),$$
$$\rho^{(2)p}\frac{\partial e^{(2)}}{\partial t}+p^{(2)p}\frac{\partial u_k}{\partial x_k}-s_{ij}^{(2)p}\frac{\partial u_j}{\partial x_i}=-l_0+u_k n_0^k+m_0\left(e^{(2)}-u^2\Big/2\right). \tag{26}$$

Using the thermodynamic identities for each phase written in the actual (non-partial) variables, the mass balance laws (20), the momentum balance laws for the phases and constitutive equations (22), from (26) we can find rates for phase entropies:

$$\rho^{(1)}T^{(1)}\frac{ds^{(1)}}{dt}=\frac{l_0+m_0\,u^2\Big/2-m_0\left(e^{(1)}+p^{(1)}\Big/\rho^{(1)}-s_{ij}^{(1)}e_{ij}^{(1)}\right)-u_k n_0^k}{\theta}+$$
$$+\frac{\rho^{(1)}\psi\left(s_{ij}^{(1)}e_{ij}^{(1)}-p^{(1)}\Big/\rho^{(1)}\right)}{\theta}+\frac{\rho^{(1)}e_{ij}^{(1)}s_{ij}^{(1)}}{\tau_1},$$
$$\rho^{(2)}T^{(2)}\frac{ds^{(2)}}{dt}=-\frac{l_0+m_0\,u^2\Big/2-m_0\left(e^{(2)}+p^{(2)}\Big/\rho^{(2)}-s_{ij}^{(2)}e_{ij}^{(2)}\right)-u_k n_0^k}{1-\theta}- \tag{27}$$
$$-\frac{\rho^{(2)}\psi\left(s_{ij}^{(2)}e_{ij}^{(2)}-p^{(2)}\Big/\rho^{(2)}\right)}{1-\theta}+\frac{\rho^{(2)}e_{ij}^{(2)}s_{ij}^{(2)}}{\tau_2}.$$

Multiplying the rate equations (27) by $\theta/T^{(1)}$ and $(1-\theta)/T^{(2)}$ and summing them up with the mass balance equations for phases multiplied by $s^{(1)}$ and $s^{(2)}$, we have

$$\frac{\partial\rho^{(1)p}s^{(1)}}{\partial t}+\frac{\partial\rho^{(1)p}s^{(1)}u_k}{\partial x_k}=$$
$$=\frac{l_0-u_k n_0^k-m_0\mu_1'}{T^{(1)}}+\frac{\rho^{(1)}\psi}{T^{(1)}}\left(s_{ij}^{(1)}e_{ij}^{(1)}-p^{(1)}\Big/\rho^{(1)}\right)+\frac{\theta\varphi_{ij}^{(1)}s_{ij}^{(1)}}{T^{(1)}}=R_1,$$
$$\frac{\partial\rho^{(2)p}s^{(2)}}{\partial t}+\frac{\partial\rho^{(2)p}s^{(2)}u_k}{\partial x_k}= \tag{28}$$
$$=-\frac{l_0-u_k n_0^k-m_0\mu_2'}{T^{(2)}}-\frac{\rho^{(2)}\psi}{T^{(2)}}\left(s_{ij}^{(2)}e_{ij}^{(2)}-p^{(2)}\Big/\rho^{(2)}\right)+\frac{(1-\theta)\varphi_{ij}^{(2)}s_{ij}^{(2)}}{T^{(2)}}=R_2.$$

Here $\mu'_k=\mu_k-u^2/2$ where μ_k is the Gibbs energy defined in the previous section.

Summing up and subtracting the equations in (28), we can obtain the entropy balance law for the averaged entropy defined in (5)

$$\frac{\partial \rho s}{\partial t} + \frac{\partial \rho s u_j}{\partial x_j} = R_1 + R_2 \,, \tag{29}$$

and the following constitutive equation for the entropy disequilibrium parameter χ defined in (9)

$$\frac{\partial \rho \chi}{\partial t} + \frac{\partial \rho \chi u_j}{\partial x_j} = R_1 - R_2 = -\rho\omega \ . \tag{30}$$

Thus, the system (17) and the constitutive equations (18), (19), (24), (25), and (30) generate a system describing behaviour of a two-phase non-dispersive strength bearing material. The conservation laws are closed with the equations of state (12) for each phase, resulting in EOS (13) for the mixture, where parameters of the phases are connected with the averaged parameters by relations (10) and (11). The constitutive equations are closed with selection of the constitutive rates (the functions φ, ψ, and ω), which will be discussed and specified in subsequent sections.

5. Constitutive Relations and EOS

Similarly to [4], we choose in the present work a brief form of a Mie-Gruneisen-type EOS suggested in [14] and modified to the set of variables in the decoupled representation:

$$e\left(\rho, e_{ij}, s\right) = \frac{a_0^2}{2\alpha_0^2} \cdot \left(\delta^{\alpha_0} - 1\right)^2 + 2\rho_0^2 b_0^2 \delta^{\beta_0+2} d + c_v T_0 \delta^{\gamma_0} \left[\exp\left(S \big/ c_v \right) - 1 \right] \ . \tag{31}$$

This EOS is used for each individual phase of the two-phase material. Here α_0, β_0, and γ_0 (Gruneisen coefficient) are material constants, c_v is the thermal capacity, ρ_0 is initial density, and $\delta = \rho/\rho_0$. It should be noted that the EOS is specific to individual phase with the phase-specific constants. The independent variables in (31) refer to $\rho^{(1)}$, $e_{ij}^{(1)}$, and $s^{(1)}$ for the first phase and to $\rho^{(2)}$, $e_{ij}^{(2)}$, and $s^{(2)}$ for the second phase. The constant a_0 is the bulk sound velocity that is linked with the longitudinal and shear sound velocities c_0 and b_0 as follows

$$a_0^2 = c_0^2 - 4b_0^2/3 \ , \tag{32}$$

and d is the second invariant of the strain deviator:

$$d = e_{ij} \cdot e_{ij} / 2 \ .$$

Shear stresses are calculated from (31) by the rule (15) as follows

$$s_{ij} = e_{e_{ij}} = e_d d_{e_{ij}} = e_d e_{ij} = 2\rho_0^2 b_0^2 \delta^{\beta_0+2} e_{ij} = 2\rho b_0^2 \delta^{\beta_0} \rho e_{ij} = 2\mu\rho e_{ij} \ , \tag{33}$$

where $\mu = \rho \cdot b^2 = \rho \cdot b_0^2 \delta^{\beta 0}$ is the shear modulus associated with the shear sound velocity b.

Similarly to [4], the relaxation time functions τ_1 and τ_2 in the constitutive equations for the strains $e_{ij}^{(1)}$ and $e_{ij}^{(2)}$ are chosen in the unified form [15]:

$$\tau(\rho, s, T) = \tau_0 \frac{\exp\left(\left(D_0 + H\varepsilon \right) \Big/ s' \right)}{N_0 + M\varepsilon} \quad . \tag{34}$$

Here τ_0, D_0, H, N_0, M are material constants that are specific to individual phases as well. The stress invariant $(s')^2 = s_{ij} \cdot s_{ij}$ and the variable ε is associated with the elastic portion of the deformation $\varepsilon = s'/(2\mu)$. The material constants are found with the routine procedure [7] employing experimental data on yield stress versus strain rate.

6. Thermodynamic Correctness of The Model

Verification of thermodynamic correctness we start with expansion of the energy conservation law in (17) reduced with the mass conservation law to the following

$$\rho \frac{de}{dt} + \rho u_i \frac{du_i}{dt} - s_{ij} \frac{\partial u_i}{\partial x_j} - u_i \frac{\partial s_{ij}}{\partial x_j} + p \frac{\partial u_k}{\partial x_k} + u_k \frac{\partial p}{\partial x_k} = 0 \ . \tag{35}$$

Using the mass and momentum conservation laws from (17) and the chain rule applied to (13), we transform the energy equation (35) as follows

$$\begin{aligned} &\rho e_\rho \frac{d\rho}{dt} + \rho e_c \frac{dc}{dt} + \rho e_\theta \frac{d\theta}{dt} + \rho e_{e_{ij}} \frac{de_{ij}}{dt} + \rho e_{\lambda_{ij}} \frac{d\lambda_{ij}}{dt} + \rho e_s \frac{ds}{dt} + \rho e_\chi \frac{d\chi}{dt} - \\ &\quad - s_{ij} \frac{\partial u_i}{\partial x_j} + p \frac{\partial u_k}{\partial x_k} = 0 \ . \end{aligned} \tag{36}$$

Using again the mass conservation law (17) and the constitutive equations (19), (18), (24), (25), and (30) for c, θ, e_{ij}, λ_{ij}, and χ, the equation (36) is reduced to the following

$$\begin{aligned} &\Lambda m_0 - \rho \Pi \psi - (\theta \varphi_{ij}^{(1)} + (1 - \theta)\varphi_{ij}^{(2)}) s_{ij} - \rho \lambda_{ij} s_{ij} \psi - (\varphi_{ij}^{(1)} - \varphi_{ij}^{(2)}) Q_{ij} + \\ &\qquad + \rho T \cdot ds/dt + (R_1 - R_2)(T^{(1)} - T^{(2)})/2 = 0 \ . \end{aligned} \tag{37}$$

In order to check out consistency of the derivation we replace the particle derivative of entropy by equation from the balance law (29) and the potentials Λ, Π, and Q_{ij} by their expressions from (16):

$$m_0(\mu^{(1)} - \mu^{(2)}) + (p^{(1)} - p^{(2)} - \rho^{(1)} e_{ij}^{(1)} s_{ij}^{(1)} + \rho^{(2)} e_{ij}^{(2)} s_{ij}^{(2)} + \rho \lambda_{ij} s_{ij}) \psi \ -$$

$$- \quad (\theta\varphi_{ij}^{(1)} + (1-\theta)\varphi_{ij}^{(2)})s_{ij} - \rho\lambda_{ij}s_{ij}\psi - (\varphi_{ij}^{(1)} - \varphi_{ij}^{(2)})\theta(1-\theta)(s_{ij}^{(1)} - s_{ij}^{(2)}) + \tag{38}$$

$$+ \quad (R_1 - R_2)\,(T^{(1)} - T^{(2)})/2 + (R_1 + R_2)\,(T^{(1)} + T^{(2)})/2 = 0\,,$$

here the corollary of the definition for Π from subsection 3 has been used. Expansion of the last two terms in (38) gives

$$R_1T^{(1)} + R_2T^{(2)} = -\,m_0(\mu^{(1)} - \mu^{(2)}) + (p^{(2)} - p^{(1)} + \rho^{(1)}e_{ij}^{(1)}s_{ij}^{(1)} - \rho^{(2)}e_{ij}^{(2)}s_{ij}^{(2)})\psi +$$

$$+ \theta\varphi_{ij}^{(1)}s_{ij}^{(1)} + (1-\theta)\varphi_{ij}^{(2)}s_{ij}^{(2)}\ .$$

Replacing the last two terms in (38) by this expansion, we obtain an identity.

In order to obtain the entropy dissipation term, we calculate the particle derivative of entropy from (37):

$$\rho T\frac{ds}{dt} = \rho\varphi\Lambda + \rho\psi\Pi + \left(\theta\varphi_{ij}^{(1)} + (1-\theta)\varphi_{ij}^{(2)}\right)s_{ij} + \rho\lambda_{ij}s_{ij}\psi +$$
$$+ \left(\varphi_{ij}^{(1)} - \varphi_{ij}^{(2)}\right)\theta(1-\theta)\left(s_{ij}^{(1)} - s_{ij}^{(2)}\right) + \rho\omega\Psi\ .$$

Expanding s_{ij} from (15) and Π from the corollary used above, we have

$$\rho T\frac{ds}{dt} = \rho\varphi\Lambda + \rho\psi\Pi_0 - \rho\lambda_{ij}s_{ij}\psi + \rho\omega\Psi + \rho\lambda_{ij}s_{ij}\psi +$$
$$+ \left(\theta\varphi_{ij}^{(1)} + (1-\theta)\varphi_{ij}^{(2)}\right)\left(\theta s_{ij}^{(1)} + (1-\theta)s_{ij}^{(2)}\right) + \left(\varphi_{ij}^{(1)} - \varphi_{ij}^{(2)}\right)\theta(1-\theta)\left(s_{ij}^{(1)} - s_{ij}^{(2)}\right)\ . \tag{39}$$

Transformation of the last two terms gives $\theta\varphi_{ij}^{(1)}s_{ij}^{(1)} + (1-\theta)\varphi_{ij}^{(2)}s_{ij}^{(2)}$. Thus, the equation (39) takes the following form

$$\rho T\frac{ds}{dt} = \rho\varphi\Lambda + \rho\psi\Pi_0 + \rho\omega\Psi + \theta\varphi_{ij}^{(1)}s_{ij}^{(1)} + (1-\theta)\varphi_{ij}^{(2)}s_{ij}^{(2)}\ . \tag{40}$$

It is easy see that the products $\varphi_{ij}^{(1)}s_{ij}^{(1)}$ and $\varphi_{ij}^{(2)}s_{ij}^{(2)}$ are proportional to $e_{ij}^{(1)}s_{ij}^{(1)}$ and $e_{ij}^{(2)}s_{ij}^{(2)}$ with positive coefficients. These terms are normally positive because the stress deviators are proportional to the strain deviators with a coefficient called the shear modulus as in (33). Thus, in order to achieve non-negative dissipation, the right-hand side of (40) can be made non-negative with the following choice of the constitutive functions φ, ψ, and ω:

$$\varphi = \Lambda\cdot\varphi_0\ , \qquad \psi = \Pi_0\cdot\psi_0\ , \qquad \omega = \Psi\cdot\omega_0\ , \tag{41}$$

where φ_0, ψ_0, and ω_0 are arbitrary nonnegative functions.

One case of practical significance is the one-dimensional plane set-up. For this case, we check out correctness separately. In this case, the system (17), (18), (19), (24), (25), (30) takes the following form:

$$\frac{\partial\rho}{\partial t}+\frac{\partial\rho u}{\partial x}=0\,,\quad \frac{\partial\rho u}{\partial t}+\frac{\partial\left(\rho u^2-s_1\right)}{\partial x}+\frac{\partial p}{\partial x}=0\,,$$
$$\frac{\partial\rho\left(e+u^2/2\right)}{\partial t}+\frac{\partial\left[\rho u\left(e+u^2/2\right)-s_1u+pu\right]}{\partial x}=0\,,$$
$$\frac{\partial\rho\theta}{\partial t}+\frac{\partial\rho\theta u}{\partial x}=-\rho\psi\,,\quad \frac{\partial\rho c}{\partial t}+\frac{\partial\rho cu}{\partial x}=-\rho\varphi\,, \tag{42}$$
$$\frac{\partial\rho e_1}{\partial t}+\frac{\partial\rho e_1u}{\partial x}-\frac{2}{3}\frac{\partial u}{\partial x}=-\left(\theta\varphi_1^{(1)}+(1-\theta)\varphi_1^{(2)}\right)-\rho\lambda_1\psi\,,$$
$$\frac{\partial\rho\lambda_1}{\partial t}+\frac{\partial\rho\lambda_1u}{\partial x}=-\left(\varphi_1^{(1)}-\varphi_1^{(2)}\right),\quad \frac{\partial\rho\chi}{\partial t}+\frac{\partial\rho\chi u}{\partial x}=-\rho\omega\ .$$

Here, the tensor component associated with the x-direction is indexed with '1' and index for vector variables associated with the same direction is omitted. Similarly to (36), using (42) for expansion of the energy equation we have

$$\rho e_c\frac{dc}{dt}+\rho e_\theta\frac{d\theta}{dt}+\rho e_{e_1}\frac{de_1}{dt}+\rho e_{\lambda_1}\frac{d\lambda_1}{dt}+\rho e_s\frac{ds}{dt}+\rho e_\chi\frac{d\chi}{dt}-s_1\frac{\partial u}{\partial x}=0\ .$$

This equation is reduced with the constitutive equations from (42) as follows

$$-e_c\varphi-e_\theta\psi+\frac{e_{e_1}}{\rho}\left[\frac{2}{3}\frac{\partial u}{\partial x}-\left(\theta\varphi_1^{(1)}+(1-\theta)\varphi_1^{(2)}\right)-\rho\lambda_1\psi\right]-\frac{e_{\lambda_1}}{\rho}\left(\varphi_1^{(1)}-\varphi_1^{(2)}\right)+T\frac{ds}{dt}-$$
$$-e_\chi\omega-\frac{s_1}{\rho}\frac{\partial u}{\partial x}=0\ . \tag{43}$$

The equation (43) gives

$$s_1=\frac{2}{3}e_{e_1}\,,\quad \frac{ds}{dt}=\frac{e_c\varphi+e_\theta\psi+e_\chi\omega+\frac{e_{e_1}}{\rho}\left[\left(\theta\varphi_1^{(1)}+(1-\theta)\varphi_1^{(2)}\right)+\rho\lambda_1\psi\right]+\frac{e_{\lambda_1}}{\rho}\left(\varphi_1^{(1)}-\varphi_1^{(2)}\right)}{T}\ . \tag{44}$$

It is easy to see that due to the tensor symmetry restrictions resulting in $d = 3e_1^2/4$, the shear stress defined in (44) is reduced to the same equation (33) in the form $s_1 = 2\mu\rho e_1$. The entropy balance equation (44) is similar to the entropy balance equation (40) in the general case, when taking into account the symmetry induced relations $s_{ij}e_{ij} = 3s_1e_1/2$ and $s_{ij}\varphi_{ij} = 3s_1\varphi_1/2$ that are valid for both the averaged and phase variables.

For checking out hyperbolicity of the system, it must be written down in the characteristic form. The present system in the corresponding form is obtained below from the system (17), (18), (19), (24), (25), and (30) as follows

$$\frac{d\rho}{dt}+\rho\frac{\partial u_k}{\partial x_k}=0\,,\quad \frac{du_i}{dt}-\frac{1}{\rho}\frac{\partial s_{ij}}{\partial x_j}+\frac{1}{\rho}\frac{\partial p}{\partial x_i}=0\,,$$
$$\frac{de_{ij}}{dt}-\frac{1}{2\rho}\left(\frac{\partial u_i}{\partial x_j}-\frac{\partial u_j}{\partial x_i}+\frac{2}{3}\frac{\partial u_k}{\partial x_k}\cdot\delta_{ij}\right)=-\frac{\left(\theta\varphi_{ij}^{(1)}+(1-\theta)\varphi_{ij}^{(2)}\right)}{\rho}-\lambda_{ij}\psi\,, \tag{45}$$
$$\frac{dc}{dt}=-\varphi\,,\quad \frac{d\theta}{dt}=-\psi\,,\quad \frac{d\lambda_{ij}}{dt}=-\frac{\left(\varphi_{ij}^{(1)}-\varphi_{ij}^{(2)}\right)}{\rho},\quad \frac{d\chi}{dt}=-\omega\,,\quad \frac{ds}{dt}=\frac{R_1+R_2}{\rho}\,.$$

It is obvious that structure of the characteristic system (45) is coincident with the structure for the single-phase background model (1) with several additional contact characteristics for eigenvectors corresponding to the trajectory evolution of variables c, θ, λ_{ij}, and χ.

Thus, the hyperbolicity conditions for the present model are identical to those from [4]:

$$p_\rho+\frac{2}{3\rho^2}\left(s_1\right)_{e_1}=a^2+\frac{4}{3}b^2=c^2\geq 0\,. \tag{46}$$

However, pressure and shear stress in (46) are calculated for the two-phase mixture using (15) and (13). Nevertheless, because of the thermodynamical correctness of the model the sound velocities are calculated with the mixture rules as described, e.g., in [6, 10]. Therefore, hyperbolicity of the system is achieved with the traditional requirement of positiveness for the expression, representing square of the longitudinal sound velocity c^2.

7. Specification of Constitutive Relations

This report is dealing with the phase transformation study for condensed two-phase materials. An essential feature of this case is that both phases are condensed if comparing with the porous materials analysed earlier when strength is neglected [6, 9]. Another feature, which differs the present case from the porous material analysis, is the combined evolution of the mass concentration due to the mass exchange driven by the phase transition and of the volume concentration due to different compressibilities of the phases. For the porous material, the mass exchange did not occur, which was tabulated by the choice $\varphi = 0$, therefore, the mass concentration did not change in a material volume [6, 9].

Because of this two-fold volume variation, we need to take into account the volume exchange due to possible phase transition. Let us consider, at a moment of time, a representative volume V of mass m for the two-phase mixture, which contains the both phases with a volume $V^{(1)}$ of the first phase material and with a volume $V^{(2)}$ of the second phase material. Corresponding masses are $m^{(1)}$ and $m^{(2)}$. In order to calculate the change of volume and mass during the phase transition process, we need to rewrite the constitutive equations for mass and volume concentrations (18) and (19) in terms of m and V as follows

$$\frac{dV^{(1)}}{dt} = -V\psi \quad , \quad \frac{dm^{(1)}}{dt} = -m\varphi \quad . \tag{47}$$

Then, the volume change $\Delta V^{(1)}$ of the first phase within a small time increment Δt is composed of the following two contributions:

$\Delta V^{(1)} = \Delta V_{\mathrm{m}}^{(1)} + \Delta V_{\mathrm{v}}^{(1)}$,

where the mass change contribution $\Delta V_{\mathrm{m}}^{(1)} = \Delta m^{(1)}/\rho^{(1)}$ is calculated from the second equation of (47):

$$\Delta m^{(1)} = \dot{m}^{(1)}\Delta t = -m\varphi\Delta t \quad , \quad \Delta V_m^{(1)} = -\frac{m\varphi\Delta t}{\rho^{(1)}} = -\frac{m\varphi\Delta t}{m^{(1)}/V^{(1)}} = -\frac{V^{(1)}\varphi\Delta t}{c}$$

and the volume change contribution $\Delta V_{\mathrm{v}}^{(1)}$ is calculated from the first equation of (47):

$\Delta V_{\mathrm{v}}^{(1)} = -V\psi\Delta t$.

Thus, the total volume change is

$$\Delta V^{(1)} = -V\psi\,\Delta t - \frac{V^{(1)}\varphi\,\Delta t}{c} \quad , \quad \frac{1}{V}\frac{\Delta V^{(1)}}{\Delta t} = -\psi - \frac{\varphi\theta}{c} = -\psi_t \quad .$$

Therefore, for a prescribed volume-change kinetic ψ driven by the description of (18), the constitutive function ψ_t associated with the total volume change is determined as follows

$\psi_t = \psi + \theta\varphi \,/\, c$,

here $\psi = \Pi_0\,\psi_0$, according to (41).

Further on, we specify the non-negative function φ_0, ψ_0, and ω_0 from (41). The function ω_0 can be selected similarly to [6, 9]:

$$\omega_0 = 2\frac{h}{\rho}\frac{T^{(1)}+T^{(2)}}{T^{(1)}T^{(2)}} \quad , \quad h = A_S\frac{k_{eff}}{d^2} \quad , \quad k_{eff} = \frac{k_1k_2}{k_2\,\theta + k_1\left(1-\theta\right)} \quad . \tag{48}$$

Here the inter-phase heat transfer coefficient h is determined according to [6, 9], d is a characteristic dimension (typical grain size for a phase), A_S is a dimensionless factor (selected as a value of the same order as previously, $A_S = 300$), and k_1, k_2 are the thermal conductivities of the phases. The function ψ_0 is chosen in the same form as [6, 9]:

$\psi_0 = \theta\,(1 - \theta)\,\theta_0(p)$. (49)

The multiplier $\theta(1 - \theta)$ keeps the parameter θ within the [0, 1] range. A function $\theta_0(p)$ responsible for the compression response is taken as

$$\theta_0(p) = A_0\left(\frac{p}{p_0}\right)^{n_0} \quad .$$

For the mass transformation rate φ_0 we take the Arrhenius kinetic:

$$\varphi_0 = B_0\left(\frac{c - c_\varepsilon}{c_{\max} - c_\varepsilon}\right)^{m_0} \cdot \frac{p}{p_0} \cdot \exp\left[-\frac{U_{act} - \gamma_s \rho_0 p}{RT}\right] \quad . \tag{50}$$

The multiplier with parameter c keeps this parameter positive with a small gap c_ε: $c > c_\varepsilon$. The constants R is the gas constant and ρ_0 is the averaged reference density.

These functions φ_0, ψ_0, and ω_0 from (48-50) will be used in the subsequent subsection for the shock wave propagation calculations.

8. Phase Transition Calculations

In the present subsection we consider an example of phase transition in pure Iron (Armco Iron) loaded by shock wave. This transition, which is usually observed statically at pressure above 11-13 GPa, is associated crystallographically with the bcc-to-hcp transition of the metal.

Table 1: Constants for the constitutive relations and EOS

EOS constants							
	ρ_0, g/cm^3	a_0, km/s	b_0, km/s	a_0	β_0	γ_0	c_v, J/g/K
α-iron	7.84	4.637	2.866	1.73	2.7	1.735	0.4415
ε-iron	8.3	4.67	3.	1.7	2.7	2.0	0.4459

Constitutive Equation constants										
k_1, W/m/K	k_2, W/m/K	A_0, g/J/s	n_0	B_0, g/J/s	m_0	d, μm	c_ε	$c_{\max}$	U_{act}, KJ/mol	γ_s, g/mol
80	50	1	1.05	3	1.5	10	0.02	0.9	26.77	0.127

Elasto-plastic transition constants				
	$d\varepsilon_1/dt$, s^{-1}	$d\varepsilon_2/dt$, s^{-1}	Y_1, GPa	Y_2, GPa
α-iron	10^{-3}	10^5	0.2	0.8
ε-iron	10^{-3}	10^5	0.8	3.2

	τ_0, s	D_0, GPa	H, GPa	N_0	M
α-iron	0.14	4.174	0	10^6	10^{11}
ε-iron	1.993	16.7	0	10^6	10^{11}

To specify EOSs for (12) in the form of (31) for α- and ε-phases, we fit constants in the EOSs to the data on α- and ε-iron published in [16, 17]. The results are summarised in Table 1. The constants chosen for the constitutive functions φ_0, ψ_0, and ω_0 of (48-50) are stated in the same Table.

The constants fitted for the elastic-plastic transition kinetic (34) are calculated from data taken for α-iron from [18] and stated as two yield limits Y_1 and Y_2 against two strain rates. The strength data for ε-iron are not common; indication of the strength increase till 3 GPa reported in [19] have been used in the Table. However, for the majority of the calculations, the same strength values have been used for the both phases except for specially stipulated cases. Initial density of the iron samples in the calculations is chosen to be $\rho_0 = 7.86$ g/cm^3.

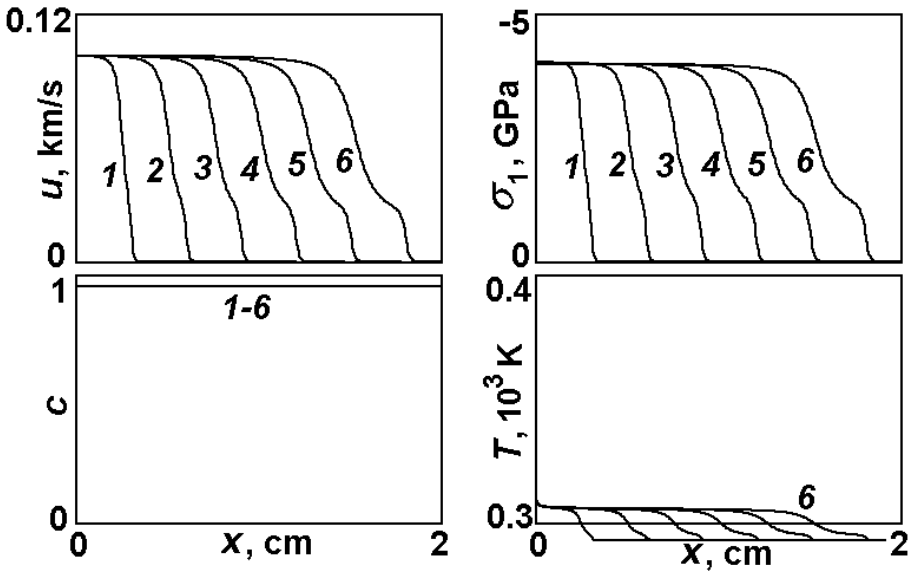

Figure 1: Evolution of shock profiles at U_0=0.1 km/s

First, the test calculations have been conducted for shock wave propagation through a 2 cm-sample for a given velocity U_0 behind the shock front. This set-up may be seen as an analysis of the target's behaviour in the plate collision one-dimensional set-up between two iron plates with the flyer plate impact velocity of $2U_0$. The variable profile in these test calculations within the sample thickness are drawn at equal intervals up to a pre-selected time T_f. The profiles are shown for velocity u, the longitudinal stress σ_1, the mass concentration of the α-phase, and temperature T.

Results of the first calculation at U_0 = 0.1 km/s are shown in Fig. 1. The final drawn profile *6* in Fig. 1 corresponds to T_f = 3.1 μsec. The calculation demonstrates that the elasto-plastic transition occurs in this case, whereas temperature varies insignificantly from its initial value T_0 = 293°K and the mass concentration does not vary at all, confirming that the α-ε-transition does not occur. The velocity and pressure profiles are quite traditional in this case and agree with many available calculations and experiments (e.g., with relevant ones published in [4]).

Next calculations shown in Figs. 2 and 3 correspond to U_0 = 0.5 km/s. Results shown in Fig. 3 were obtained with the strength data for ε-phase taken from Table 1. The shock profiles in these calculations evolve till T_f = 3.3 μsec.

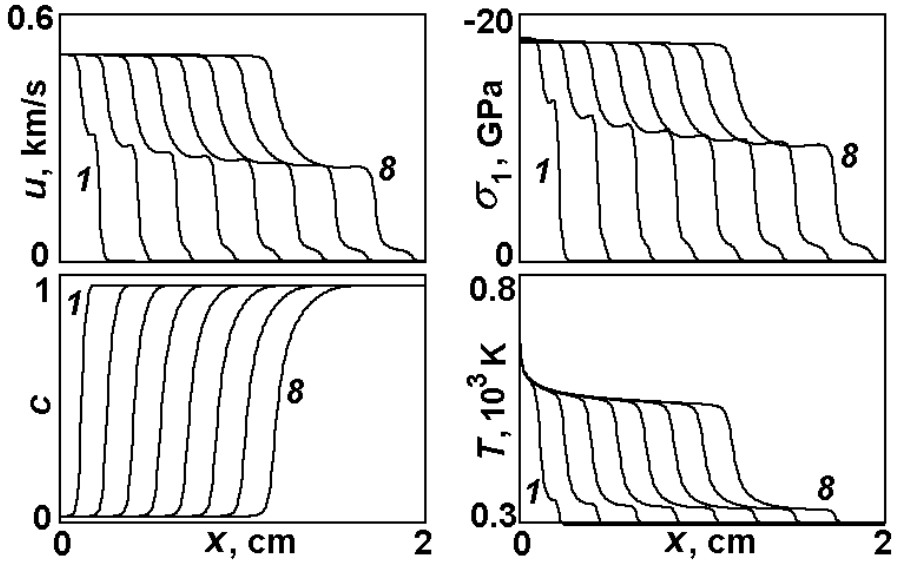

Figure 2: Evolution of shock profiles at U_0=0.5 km/s

The calculations show that both elasto-plastic and phase transitions take place in this case.

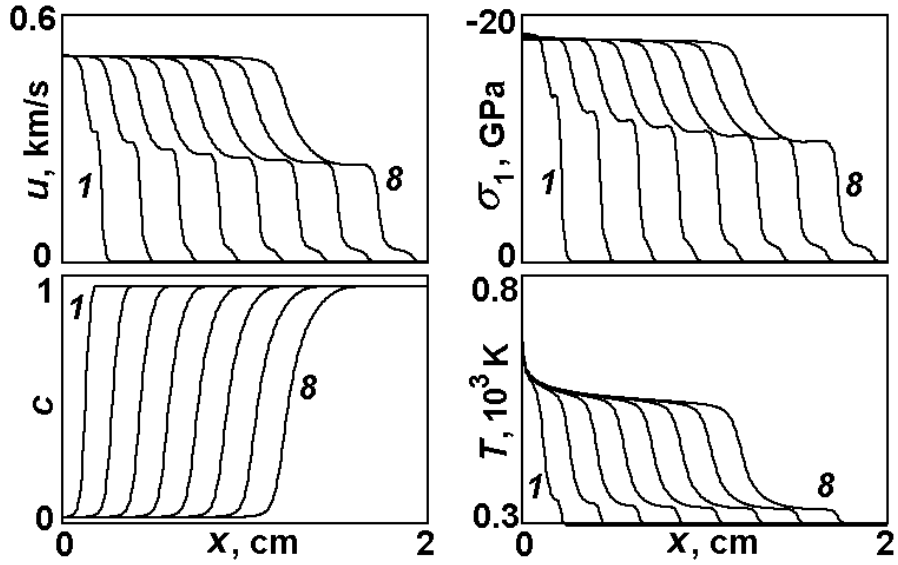

Figure 3: Evolution of shock profiles at U_0=0.5 km/s. The strength of ε-phase is elevated.

It is seen that the strength elevation of the high-pressure ε-phase does influence the profiles, although, not very significantly. As in the previous calculation, the elasto-plastic transition does not result in an essential temperature change and, naturally, gives no mass concentration change. The mass concentration change occurs mainly within the second transition (α-ε-transition). Thus, typical three-wave structure is observed at this level of

load. It is interesting to note that the profile evolution, when developing the phase transition within the shock wave with time, manifests a well-known attenuation of the particle velocity and pressure behind the phase-transformation step. Discussion on this topic can be found, for example, in [20].

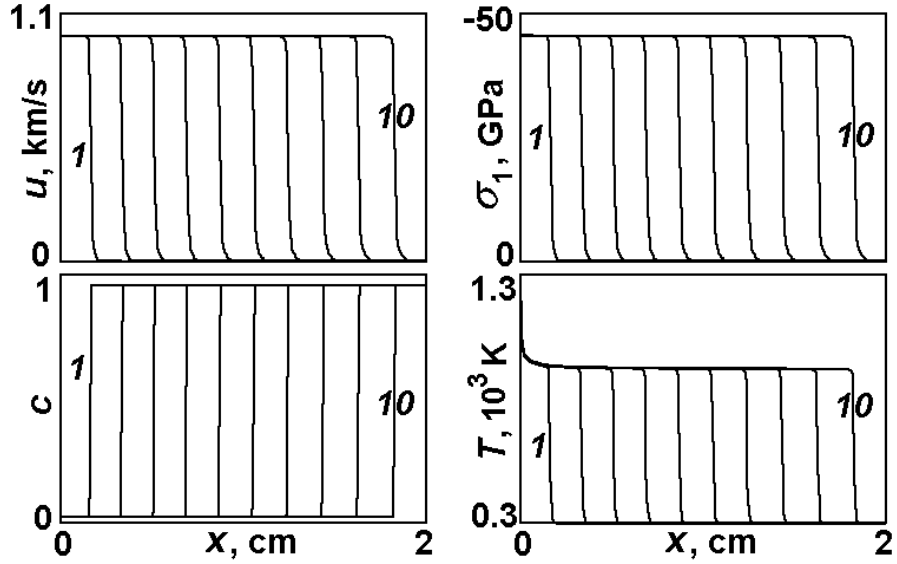

Figure 4: Evolution of shock profiles at U_0=1 km/s

Results of the last calculation of this series at U_0 = 1 km/s is shown in Fig. 4 (T_f = 3.2 μsec). In this case, the wave velocity of the phase-transforming step, while increasing with U_0, exceeds the wave velocity of the preceding steps and the three-wave structure degenerates into a single-wave shock wave within which both elasto-plastic and α-ε-transitions take place.

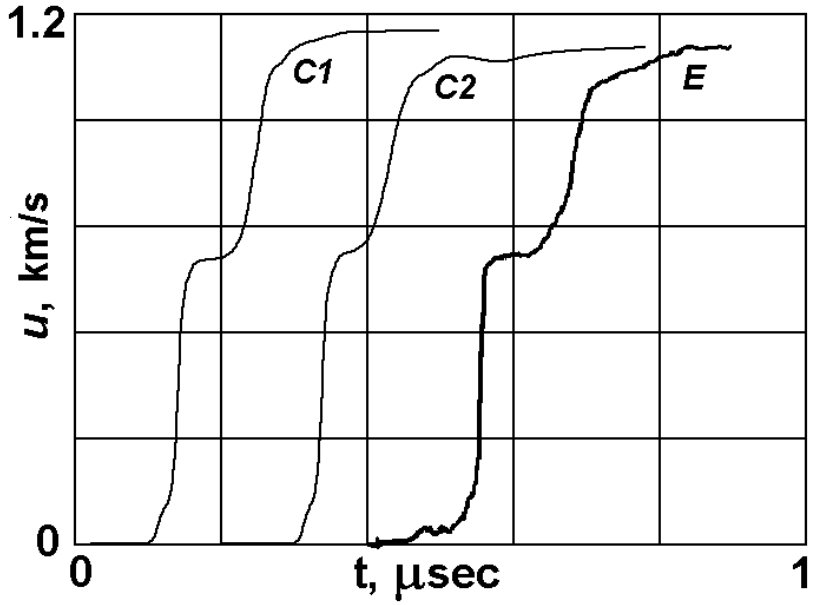

Figure 5: Free surface velocity profiles at high velocity impact by Aluminium plate

Last calculations aim at validation of the model. First calculation set-up corresponds to an experiment conducted in [21] for high velocity impact of 2.46 mm-target made from Iron by 2 mm Aluminium flyer plate. The impact velocity is 1.9 km/s. Calculation of behaviour of the Aluminium plate is conducted with the model and data taken from [4]. The profiles drawn in Fig. 5 correspond to the free surface velocity of the target taken with use of Laser Interferometry (the VISAR technique). Profile *E* in Fig. 5 is an experimental one taken from [21], profile *C1* is calculated with the EOS and constitutive relation data used in the test calculations above, and profile *C2* is calculated with the elevated strength similarly to the calculation in Fig. 3. An extended forerunner in front of the elastic precursor of the profile *E* is explained in [21] by the influence of an attached air shock being developed in the test. It is seen from Fig. 5 that the maximum velocity that is mainly affected by properties of the ε-phase is slightly changed when comparing *C1* and *C2*, but the change is not dramatic (although *C2* agrees better with the experiment *E*).

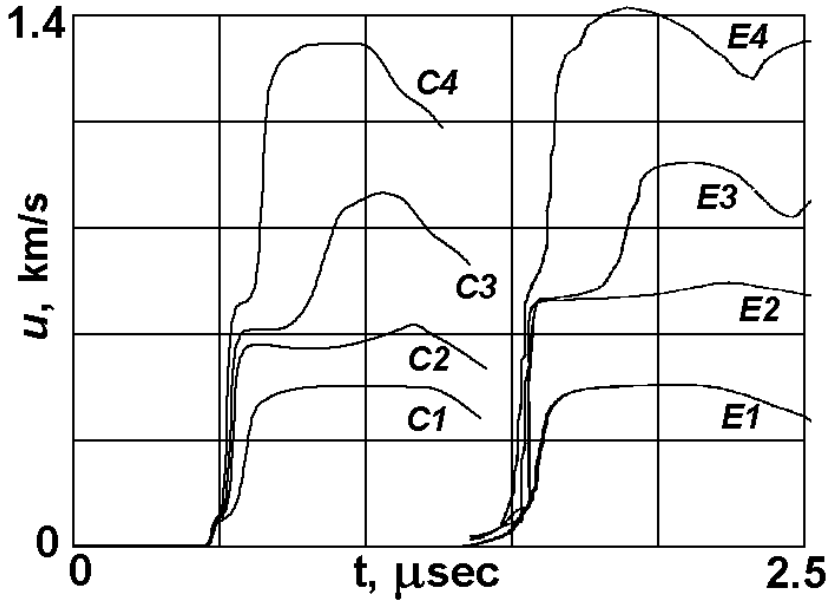

Figure 6: Free surface velocity profiles at high velocity symmetric impact by Iron plate

The last calculation is conducted for several impact velocities in the symmetric collision set-up between 2 mm iron flyer plate and 4mm iron target. The target's free surface velocities are recorded [22] in the same fashion as in the test [21]. The impact velocities are: 1) 437 m/s; 2) 779 m/s; 3) 1079 m/s; and 4) 1457 m/s. The corresponding experimental profiles (*E1-E4*) taken from [22] and calculated profiles (*C1-C4*) are shown in Fig. 6. The calculation shows a good agreement and a pleasing description of the kinetic features associated with the wave degeneration when impact velocity is increasing.

9. Conclusions

The present work has generalised the decoupled strength model [4] for the case of two-phase non-dispersive materials. In doing so, the decoupling principle was preserved that will allow implementation of the model in commercial hydrocodes. Thermodynamic correctness of the model has been established and conditions of the correctness formulated.

Relations for the constitutive equations of the model have been built up for Iron and a kinetic of the bcc-to-hcp phase transition of Iron described. The model has been validated, using experimental data on the α-ε-phase transition available in literature. Kinetic behaviour of the elasto-plastic and phase transition resulting in a three-wave structure corresponding to both transitions has been observed in the calculations using the model.

References

1. Hallquist, J.O., Stillman D.W., and Lin T-L., "LS-DYNA3D User's Manual", Livermore Software Technology Corporation, Livermore, CA, 1994.
2. Bell R.L., Baer M.R., Brannon R.M., Crawford D.A., Elrick M.G., Hertel E.S. Jr., Schmitt R.G., Silling S.A., and Taylor P.A., "CTH user's manual and input instructions version 7.1," Sandia National Laboratories, Albuquerque, NM, 2006.
3. Godunov S.K. and Romenskii E.I., "Elements of Continuum Mechanics and Conservation Laws", Kluwer Academic Publ., N.Y., 2003.
4. Resnyansky A.D., Thermodynamically Consistent Decoupled Shear-Volumetric Strain Model and CTH Implementation, DSTO Report DSTO-TR-2299, Edinburgh, SA, Australia, 2009.
5. Godunov S.K., Zabrodin A.V., Ivanov M.Ya., Kraiko A.N., and Prokopov G.P., "Numerical Solution of Multi-Dimensional Problems of Gas Dynamics," Nauka Press, Moscow, 1976 [in Russian] (French transl: "Résolution Numérique des Problémes Multidimensionnels de la Dynamique des Gaz," Mir, Moscow, 1979).
6. Resnyansky A.D., Constitutive Modeling of Hugoniot for a Highly Porous Material, J. Appl. Physics, 2008, v. 104, n. 9, pp. 093511-14.
7. Resnyansky A.D., DYNA-modelling of the high-velocity impact problems with a split-element algorithm, Int. J. Impact Eng., 2002, v. 27, n. 7, pp. 709-727.
8. Resnyansky A.D., Constitutive modelling of the shock behaviour of a highly porous material, DSTO Report DSTO-TR-2026, Edinburgh, SA, Australia, 2007.
9. Resnyansky A.D., Hugoniots of Porous Materials at Non-Equilibrium Conditions, DSTO Report DSTO-TR-2137, Edinburgh, SA, Australia, 2008.
10. Resnyansky A.D. and Bourne N.K., Shock-wave compression of a porous material, J. Appl. Physics, 2004, v. 95, n. 4, pp. 1760 - 1769.

11. Resnyansky A.D., Romensky E.I., and Bourne N.K., Constitutive Modeling of Fracture Waves, J. Appl. Physics, 2003, v. 93, n. 3, pp. 1537-1545.

12. Resnyanskii A.D. and Romenskii E.I., Dynamic strain model for a fibrous thermoviscoelastic composite, Comb., Expl., Shock Waves, 1992, v. 28, n. 4, pp. 430-436.

13. Resnyanskii A.D. and Romenskii E.I., Model of dynamic deformation of a laminated thermoviscoelastic composite, Comb., Expl., Shock Waves, 1993, v. 29, n. 4, pp. 535-541.

14. Dorovskii V.N., Iskol'dskii A.M., and Romenskii E.I., Dynamics of impulsive metal heating by a current and electrical explosion of conductors, J. Appl. Mech. Techn. Phys., 1983, v. 24, n. 4, pp. 454-467.

15. Merzhievsky L.A. and Resnyansky A.D., Dislocation structure in the models of dynamic deformation and fracture of metals, J. de Physique, 1985, v. 46, Suppl. n. 8, Coll C5, pp. 67-72.

16. Andrews D.J., Equation of State of the Alpha and Epsilon Phases of Iron, J. Phys. Chem. Solids, 1973, v. 34, n. 5, pp. 825-840.

17. Yano K. and Horie Y., Mesomechanics of the α-ε transition in iron, Int. J. Plasticity, 2002, v. 18, n. 11, pp. 1427-1446.

18. Campbell J.D. and Ferguson W.G., The temperature and strain-rate dependence of the shear strength of mild steel, Philos. Mag., 1970, v. 21, n. 169, pp. 63-82.

19. Armstrong R.W., Arnold W., and Zerilli F.J., Dislocation mechanics of copper and iron in high rate deformation tests, J. Appl. Phys., 2009, v. 105, n. 2, pp. 023511-7.

20. Hayes D.B., Kinetics of shock-induced polymorphic phase transitions, Sandia National Laboratories Report SAND-77-0267C, Albuquerque, NM, 1976.

21. Kanel G.I., Razorenov S.V., and Fortov V.E., Shock-wave compression and tension of solids at elevated temperatures: superheated crystal states, pre-melting, and anomalous growth of the yield strength, J. Phys.: Condens. Matter, 2004, v. 16, n. 14, pp. S1007-S1016.

22. Buy F., Voltz Ch., Heuzé O., and Missonnier M., Role of the α-ε transition on the damage patterns of iron, 2006, J. Phys. IV France , v. 134, pp. 263-268.

DEFENCE SCIENCE AND TECHNOLOGY ORGANISATION
DOCUMENT CONTROL DATA

1. PRIVACY MARKING / CAVEAT (OF DOCUMENT)

2. TITLE

Thermodynamically Consistent Decoupled Strength Model for Two-Phase Materials with Phase Transitions

3. SECURITY CLASSIFICATION (FOR UNCLASSIFIED REPORTS THAT ARE LIMITED RELEASE USE (L) NEXT TO DOCUMENT CLASSIFICATION)

Document	(U)
Title	(U)
Abstract	(U)

4. AUTHOR(S)

A.D. Resnyansky

5. CORPORATE AUTHOR

DSTO Defence Science and Technology Organisation
PO Box 1500
Edinburgh South Australia 5111 Australia

6a. DSTO NUMBER	6b. AR NUMBER	6c. TYPE OF REPORT	7. DOCUMENT DATE
DSTO-TR-2367	AR-014-677	Technical Report	December 2009

8. FILE NUMBER	9. TASK NUMBER	10. TASK SPONSOR	11. NO. OF PAGES	12. NO. OF REFERENCES
	LRR 07 / 249	DSTO	21	22

13. URL on the World Wide Web

http: / / www.dsto.defence.gov.au / corporate / reports / DSTO-TR-2367.pdf

14. RELEASE AUTHORITY

Chief, Weapons Systems Division

15. SECONDARY RELEASE STATEMENT OF THIS DOCUMENT

Approved for public release

OVERSEAS ENQUIRIES OUTSIDE STATED LIMITATIONS SHOULD BE REFERRED THROUGH DOCUMENT EXCHANGE, PO BOX 1500, EDINBURGH, SA 5111

16. DELIBERATE ANNOUNCEMENT

No Limitations

17. CITATION IN OTHER DOCUMENTS Yes

18. DSTO RESEARCH LIBRARY THESAURUS http: / / web-vic.dsto.defence.gov.au / workareas / library / resources / dsto_thesaurus.shtml

Constitutive Two-Phase Model; Strength; Shock Waves; Thermodynamics; Phase Transitions.

19. ABSTRACT

A constitutive two-phase material model is formulated, which satisfies the decoupling of deviatoric stress and pressure response required by many hydrocodes. Two-phase materials are assumed to be non-dispersive. Basis of the present model is a decoupled model based on a general Maxwell-type viscoelastic model. The proposed formulation provides thermodynamic consistency for the case of small elastic shear strains and unrestricted volumetric response. The model is verified against experimental data on the shock wave propagation in iron resulting in alpha-epsilon phase transition, while the strength effects being observed at the same time.